Figure 2. Velocity-resolved emission centroids across the double-peaked Brγ "stationary" line for observations in 2016 (left) and 2017 (right). The emission centroid of the spatially resolved baryonic jets is also shown. The black circles correspond to the estimated binary orbit size.

The spectral differential visibilities measured by GRAVITY (GRAVITY Collaboration et al., 2017a) reveal an extended wind with a size several times the stellar radius, which is also significantly distorted — being more extended on the side that is shielded from the pulsar — and which could be caused by the X-ray ionisation of the stellar wind facing the compact object. In addition, asymmetries revealed by the differential visibility phases across the emission lines may point to an additional component, possibly a stream of enhanced density which has been posited to exist in the system from the analysis of X-ray light curves (Leahy & Kotska, 2008). Further observations at different orbital phases could take advantage of the significant eccentricity in order to disentangle intrinsic variability of the wind from the distortion caused by the pulsar accretion.

References

Blondin, J. M. 1994, ApJ, 435, 756
Blundell, K. et al. 2001, ApJ, 562, L79
Fabrika, S. 2004, Space Science Reviews, 12, 1
GRAVITY Collaboration et al. 2017a, ApJ, 844, 177
GRAVITY Collaboration et al. 2017b, A&A, 602, L11
Kaper, L. et al. 2006, A&A, 457, 595
Leahy, D. & Kostka, M. 2008, MNRAS, 384, 747
Margon, B. et al. 1979, ApJ, 233, L63
Milgrom, M. 1979, A&A, 78, L9
Waisberg, I. et al. 2019a, A&A, 623, A47
Waisberg, I. et al. 2019b, A&A, 624, A127

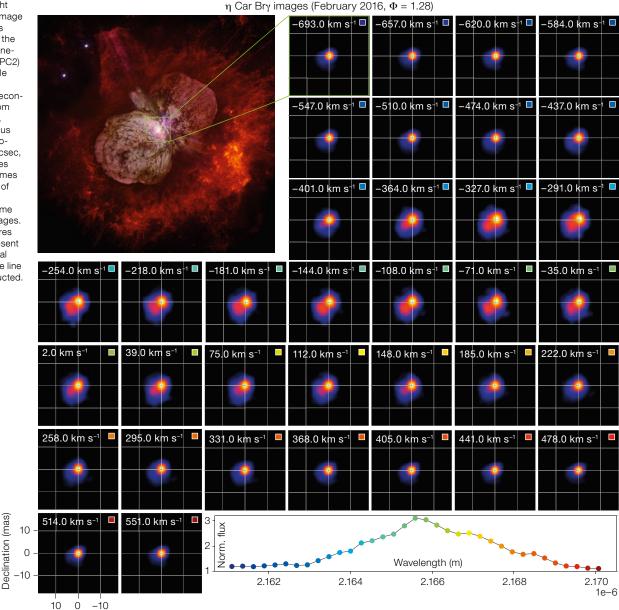# Images at the Highest Angular Resolution with GRAVITY: The Case of η Carinae

GRAVITY Collaboration (see page 20)

The main goal of an interferometer is to probe the physics of astronomical objects at the highest possible angular resolution. The most intuitive way of doing this is by reconstructing images from the interferometric data. GRAVITY at the Very Large Telescope Interferometer (VLTI) has proven to be a fantastic instrument in this endeavour. In this article, we describe the reconstruction of the wind-wind collision cavity of the massive binary η Car with GRAVITY across two spectral lines: HeI and Brγ.

Interferometric imaging

With a resolving power that is a factor of tens of times better than stand-alone telescopes, infrared interferometry offers the possibility to produce milliarcsecond (mas) resolution images. Therefore, interferometric imaging is a key means to acquire information addressing a broad range of astronomical problems, ranging from the detection of planets to mapping the cores of active galactic nuclei (AGN).

Interferometers reach a level of detail proportional to the separation between each pair of telescopes in the array, known as baselines. Baselines record information, at a given orientation, of the brightness distribution of the object on the sky. Interferometric observables, called visibilities, are a series of Fourier (spatial) frequencies. These frequencies correspond to different levels of detail in the image. The highest frequencies trace the finest

Figure 1. Upper-right panel: Composite image of the "Homunculus Nebula" taken with the Wield Field and Planetary Camera 2 (WFPC2) on board the Hubble Space Telescope. Small panels: Brγ reconstructed images from the Feb. 2016 data. With the Homunculus Nebula having a projected size of 17 arcsec, the GRAVITY images represent an 850 times zoom into the core of η Car. The Doppler velocity of each frame is labeled in the images. The coloured squares in the images represent the different spectral channels across the line that were reconstructed.
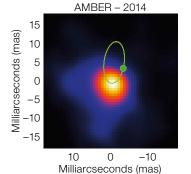
η Car Brγ images (February 2016, Φ = 1.28)

textures (like granular surfaces, or point-like objects) while the lowest ones trace extended textures (like edges and contours). An image is, therefore, composed of an infinite number of frequencies. However, interferometers only sample a few of them.
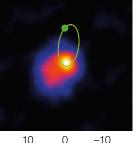
Thus, recovering an image from interferometric data is an "ill-posed" problem with more unknowns (pixels in the image) than constraints (data). Reconstructing images requires the use of iterative regularised least-squares minimisation algorithms.

These algorithms minimise (i) the difference between the data and the visibilities obtained from the model image (i.e., the likelihood term), and (ii) the value of one or several priors (i.e., the regularisers), which are defined based on the knowledge of the source (see Sanchez-Bermudez et al., 2018). Reconstruction packages available to the community optimise through gradient-descent (for example, MiRA: Thiébaut, 2008; BSMEM: Buscher, 1994) or Monte-Carlo Markov-Chain methods (for example, SQUEEZE: Baron & Kloppenborg, 2010).

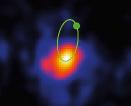## The massive binary at the core of η Car

Located at the core of the "Homunculus Nebula" (see Figure 1) at a distance of 2.3 kiloparsecs, η Car is a very massive and intriguing object. Indirect observations suggest that a binary with a period of 5.54 years resides in its core. The primary, η_A, is supposedly a star with a mass of around 100 $M_\odot$, while the secondary, η_B, appears to be a hotter star, perhaps a giant O-star, with a mass of around 30 $M_\odot$, but around 100 times fainter than the primary. Different observations suggest that

| AMBER – 2014 | GRAVITY – 2016 | GRAVITY – 2018 |

Figure 2. Comparison between the wind-wind collision zone's morphologies at different orbital phases of η_B taken with AMBER (2014) and GRAVITY (2016, 2018) at a Doppler (blue-shifted) velocity of -280 km s^{-1}. The projected trajectory of the secondary and its position are marked by the green ellipse and dot, respectively, in each of the panels. Notice how the structure of the cavity changes considerably depending on the secondary's orbital phase. For example, the south-eastern clump observed in 2016 disappears in the 2018 reconstruction.

η_A exhibits a very dense and slow wind that shocks with a much faster and lighter wind from the secondary.

The existence of η_B produces several changes in the morphology of η_A's wind. In particular, it photoionises part of the primary wind, changing the strength of lines such as Hα, He I, Fe II, or Ne II (Mehner et al., 2010, 2012; Madura et al., 2012). 2D radiative transfer models and 3D hydrodynamical simulations of the wind-wind collision scenario suggest that the high-velocity secondary wind penetrates the slow and dense primary wind creating a low-density cavity in it, with thin and dense walls where the two winds interact (Madura et al., 2013; Clementel et al., 2015a,b).

Several attempts have been made to map the core of η Car and to peer into the structure of the wind-wind collision region, and of the binary itself, at scales of 5–10 astronomical units (au) or 2–4 mas. Long-baseline infrared interferometry has been a decisive technique for such studies (van Boekel et al., 2003; Weigelt et al., 2007). Astronomical Multi-BEam combineR (AMBER) observations in 2014 allowed, for the first time, the recovery of aperture-synthesis images, at a resolution of ~ 6 mas of the wind-wind collision cavity across Brγ (Weigelt et al., 2016).

Observing η Car with GRAVITY

The unique characteristics of η Car make it a good candidate for increasing our understanding of the role of multiplicity in shaping the fate of stars at the upper end of the Initial Mass Function (IMF). It

was therefore selected as a target for the Guaranteed Time Observations (GTO) GRAVITY programme (GRAVITY Collaboration, 2017), with the objective of carrying out a long-term (monitoring) analysis of the wind-wind collision cavity through interferometric imaging.

The first reconstructed images, presented in GRAVITY Collaboration (2018), included data taken during the commissioning phase (in 2016) of GRAVITY and through regular P100 programmes (in 2017). η Car was observed with the Auxiliary Telescopes (ATs) using the high-spectral-resolution mode of GRAVITY. This setup allowed us to resolve several spectral lines across the target's spectrum and thereby to monitor the morphologies of the core at different Doppler velocities. In particular, we focused our efforts on mapping Brγ and the He I 2s–2p lines.

Images were recovered using SQUEEZE. Prior information necessary for the reconstruction was included in both the spatial and spectral domains to obtain simultaneous images of 35 different spectral channels, with a resolution as good as 1.75 mas (4 au; see Figure 1). Compared with the 2014 AMBER images, the GRAVITY Brγ ones revealed structural changes associated with the orbital motion of the secondary. In particular, a bright "clump" is observed towards the southeast of the central core, which was identified as part of shocked wind flowing along the inner cavity walls after the last η_B periastron in 2014.

The He I images revealed, for the first time, the distribution of this element in η Car's core. We suggest that the partially

ionised He I is formed from (i) a portion of the primary wind, which is photoionised by the strong ultraviolet radiation of the η_B wind, and (ii) by the shocked material in the cavity walls. To properly quantify this scenario new spectro-interferometric images are required in combination with dedicated modelling. Two additional imaging epochs in 2018 and 2019 have been obtained with GRAVITY. From the preliminary analysis of data taken in 2018, we can confirm that the morphology of the wind-wind collision zone changes depending on the orbital phase of the secondary (Figure 2). As demonstrated in the case of η Car, GRAVITY spectro-interferometric imaging provides unique information that can help to characterise the physics associated with the morphology of complex systems at the highest angular resolution currently possible in the near-infrared.

References

Baron, F. & Kloppenborg, B. 2010, Proc. SPIE, 7734, 77344D
Buscher, D. F. 1994, *Very High Angular Resolution Imaging*, IAU Symposium, 158, 91
Clementel, N. et al. 2015a, MNRAS, 450, 1388
Clementel, N. et al. 2015b, MNRAS, 447, 2445
GRAVITY Collaboration 2017, A&A, 602, A94
GRAVITY Collaboration 2018, A&A, 618, 125
Mehner, A. et al. 2010, ApJ, 710, 729
Mehner, A. et al. 2012, ApJ, 751, 73
Madura, T. I. et al. 2012, ApJ, 647, L18
Madura, T. I. et al. 2013, MNRAS, 436, 3820
Sanchez-Bermudez, J. et al. 2018, Experimental Astronomy, 46, 457
Thiébaut, E. 2008, Proc. SPIE, 7013, 701311
van Boekel, R. et al. 2003, A&A, 410, L37
Weigelt, G. et al. 2007, A&A, 464, 87
Weigelt, G. et al. 2016, A&A, 594, A106